ARTICLE

Circulating small extracellular vesicles promote proliferation and migration of vascular smooth muscle cells via AXL and MerTK activation

Young Joo Lee[1], Miso Park[1], Hyun Young Kim[1], Jin-Ki Kim[2], Won-Ki Kim[3], Sung Chul Lim[4] and Keon Wook Kang[1]

The proliferation and migration of vascular smooth muscle cells (VSMCs) after vascular injury lead to neointimal hyperplasia, thus aggravating vascular diseases. However, the molecular mechanisms underlying neointima formation are not fully elucidated. Extracellular vesicles (EVs) are mediators of various intercellular communications. The potential of EVs as regulators in cardiovascular diseases has raised significant interest. In the current study we investigated the role of circulating small extracellular vesicles (csEVs), the most abundant EVs (10^{10} EVs/mL serum) in VSMC functions. csEVs were prepared from bovine, porcine or rat serum. We showed that incubation with csEVs ($0.5 \times 10^{10}-2 \times 10^{10}$) dose-dependently enhanced the proliferation and migration of VSMCs via the membrane phosphatidylserine (PS). In rats with ligation of right carotid artery, we demonstrated that application of csEVs in the ligated vessels aggravated neointima formation via interaction of membrane PS with injury. Furthermore, incubation with csEVs markedly enhanced the phosphorylation of AXL and MerTK in VSMCs. Pretreatment with BSM777607 (pan-TAM inhibitor), bemcentinib (AXL inhibitor) or UNC2250 (MerTK inhibitor) blocked csEV-induced proliferation and migration of VSMCs. We revealed that csEV-activated AXL and MerTK shared the downstream signaling pathways of Akt, extracellular signal-regulated kinase (ERK) and focal adhesion kinase (FAK) that mediated the effects of csEVs. We also found that csEVs increased the expression of AXL through activation of transcription factor YAP, which might constitute an AXL-positive feedback loop to amplify the signals. Finally, we demonstrated that dual inhibition of AXL/MerTK by ONO-7475 (0.1 μM) effectively hindered csEV-mediated proliferation and migration of VSMCs in ex vivo mouse aorta injury model. Based on these results, we propose an essential role for csEVs in proliferation and migration of VSMCs and highlight the feasibility of dual AXL/MerTK inhibitors in the treatment of vascular diseases.

Keywords: vascular smooth muscle cells; circulating small extracellular vesicles; neointimal hyperplasia; phosphatidylserine; AXL; MerTK; BSM777607; bemcentinib; UNC2250; ONO-7475

INTRODUCTION

Neointimal hyperplasia is a key process in restenosis after percutaneous transluminal angioplasty (PTA). Balloon inflation or stent insertion during PTA imposes mechanical stress on the vascular wall, resulting in abnormal proliferation and migration of vascular smooth muscle cells (VSMCs), and ultimately leading to restenosis [1]. When the endothelial wall is damaged, VSMCs are exposed to growth factors and cytokines secreted by activated macrophages, platelets and endothelial cells [2]. To support vascular recovery, VSMCs migrate across the internal elastic lamina to the intimal region, where they proliferate to form a new intimal layer, the neointima. This is the process by which neointimal hyperplasia narrows the vascular lumen and, thus, aggravates vascular diseases [3–5]. However, the precise mechanism(s) of neointima formation has yet to be fully elucidated, and so inhibition of excessive proliferation and migration of VSMCs after interventions in vascular diseases remains a major challenge.

Small extracellular vesicles (sEVs) are phospholipid bilayer membrane vesicles of 30–200 nm diameter [6]. sEVs contain proteins, lipids, and microRNA (miR), the amounts of which vary depending on the parent cells [7]. Recent studies have shown that sEVs play a pivotal role in intercellular signaling, by transporting cargos or interacting with membrane proteins [8]. With sEVs' emergence as a key mediator in intercellular signaling, their role in cardiovascular diseases has been extensively explored. Recent studies have suggested that sEVs derived from peripheral cells or specific disease states function as a modulator of VSMC phenotypes. In one of these studies, macrophages accumulated in the injured vascular area released sEVs to increase the proliferation and motility of VSMCs [9]. Elsewhere, sEVs from activated platelets were reported to induce pro-inflammatory VSMC phenotypes [10]. In a third study, sEVs from the plasma of patients with peripheral artery disease were found to increase VSMC migration [11].

[1]College of Pharmacy and Research Institute of Pharmaceutical Sciences, Seoul National University, Seoul 08826, Republic of Korea; [2]College of Pharmacy, Hanyang University, Gyeonggi-do 15588, Republic of Korea; [3]Department of Neuroscience, Korea University College of Medicine, Seoul 02841, Republic of Korea and [4]Department of Pathology, Medical school, Chosun University, Gwangju 61453, Republic of Korea
Correspondence: Keon Wook Kang (kwkang@snu.ac.kr)

csEVs promote proliferation and migration of VSMCs
YJ Lee et al.

985

The discovery that sEVs of various origins exert effects on VSMCs prompted us to clarify circulating sEVs' (csEVs') capability of modulating VSMCs. csEVs are present in the blood at very high concentrations measured to more than 10^{10} per 1 mL of serum, even allowing for variation depending on the methods of separation and measurement [12]. csEVs face difficulty in passing through the vascular wall, due to vascular endothelial cells that tightly line the inner surface of normal blood vessels. However, vascular damage widens the gaps between endothelial cells, generating an environment in which csEVs can succeed in penetrating the vascular wall and affecting VSMCs [13]. In this regard, we recently showed that csEVs strongly induce migration of cancer cells via TYRO3 activation [14]. TAM receptor family (TYRO3/AXL/MerTK) is a well-known PS-sensing receptor family [15]. In particular, AXL is highly expressed in VSMCs from injured vessels and mediates their proliferation and survival [16]. The phosphatidylserine (PS) lipid moiety, which is abundant in the csEV membrane, is required to fully activate the TAM receptor family. Therefore, in this study, we sought to establish whether csEVs induce changes in VSMC functions and, if so, to determine whether the csEV-VSMC interaction involves TAM receptors.

MATERIALS AND METHODS
Isolation of vascular smooth muscle cells
VSMCs were isolated from the thoracic aorta of 8 weeks old Sprague-Dawley (SD) rat and C57BL/6 mice for primary culture. In brief, the connective tissue of thoracic aorta was removed in Hank's balanced salt solution (HBSS) with fine tweezers under microscope. The tissue was incubated in HBSS containing 2000 U type 2 collagenase for 10 min. The adventitia was removed in HBSS under microscope. The tissue was incubated overnight at 37 °C in 5% CO_2, Dulbecco's modified Eagle's medium supplemented with 10% fetal bovine serum (FBS) and 1% penicillin/ streptomycin. The tissue was transferred to HBSS containing 2000 U type 2 collagenase and 1.5 U elastase. The aorta was laterally minced into small pieces with scalpels and incubated in 37 °C for 45 min. The digested tissues were dissociated to single cells and centrifuged at $300 \times g$ for 5 min. The isolated VSMCs were resuspended in Dulbecco's modified Eagle's medium (DMEM) supplemented with 10% FBS and 1% penicillin/strepto-mycin. VSMCs with passage number 2 to 9 were used in the experiments.

Total ligation of right carotid artery model
Seven weeks old male SD rats were obtained from Raon Bio (Seoul, Republic of Korea) and acclimatized for 1 week prior to surgery. SD rats were anesthetized with 3.5% isoflurane in 2:1 N_2O/O_2 mixture in an anesthesia chamber. The anesthesia was sustained through a nasal cone with 2.5% isoflurane. The right common carotid artery just below the bifurcation of external carotid artery and internal carotid artery was ligated twice with 4-0 silk suture. After ligation, 100 μL of 25% F-127 gel preloaded with vehicle, csEV or PS liposome (150 μg/mL) was applied to the ligated vessels. The rats with ligated artery were fed with atherogenic rodent diet (D12336, Research Diets, NJ, USA) for 2 weeks, and sacrificed to obtain the operated carotid arteries. The ligated region of arteries was formalin-fixed paraffin-embedded (FFPE). Serial axial sections of 4 μm thickness of FFPE tissue blocks were prepared. The sections were stained with hematoxylin and eosin and scanned under the fluorescence microscope (Olympus IX70). The area between the luminal circumference and the internal elastic lamina was measured as neointimal area. The area between the internal and external elastic lamina was defined as media. The area of the neointima divided by the area of the media was defined as the neointima/media ratio. The animal experimental procedure was approved by IACUC (Institutional Animal Care and Use Committee, SNU-210215-2) in Seoul National University.

Ex vivo artery injury model
Eight weeks old male C57BL/6 mice were obtained from Raon Bio (Seoul, Republic of Korea) and acclimatized for 1 week prior to surgery. Mice were anesthetized via intraperitoneal injection of Zoletil®50 (30 mg/kg, Virbac Laboratories, Carros, France) and Rompun® (10 mg/kg, Bayer Korea, Republic of Korea). The descending thoracic aorta was dissected and placed in ice-cold DPBS. The connective tissues were removed with fine forceps. For removal of the endothelial layer, aortas were flushed with 0.25% trypsin EDTA (Gibco, Waltham, MA, USA) and DPBS consecutively. Media was injured by inserting a 24-gauge sterile needle into the aortas. The isolated aortas were cut into two sections respectively and cultured with indicated substances in DMEM supplemented with 10% EV-free FBS and 1% penicillin/streptomycin in 12-well plate for 5 days. FFPE tissue blocks and hematoxylin and eosin-stained sections of the injured aortas were prepared and scanned as described in total ligation of right carotid artery model. The animal experimental procedure was approved by IACUC (Institutional Animal Care and Use Committee, SNU-210907-3) in Seoul National University.

Antibodies and reagents
Antibodies recognizing AXL (ab215205), MerTK (ab14920), and p-YAP (Y357, ab62751) were purchased from Abcam (Cambridge, UK). TYRO3 (5585 S), p-AXL/MerTK/TYRO3 (44463 S), anti-rabbit IgG (7074 S), anti-mouse IgG (7076 S), YAP (8418 S), p-FAK (3283 S), p-Akt (9271 S), Akt (9272 S), p-mTOR (5536 S), mTOR (2983 S), p-S6K (9234 S), and S6K (9202 S) antibodies were purchased from Cell Signaling Technology (Danvers, MA, USA). Anti-GAPDH antibody (CB1001) was supplied from Millipore (Burlington, MA, USA). CD63 (sc-5275) was obtained from Santa Cruz Biotechnology (Dallas, CA, USA). Bovine CD63 (MCA2042GA) was purchased from Bio-Rad (Hercules, CA, USA). Bovine serum (16170-078), porcine serum (26250084), and Alexa Fluor 488 goat anti-Rabbit IgG (A11034) were purchased from ThermoFicher Scientific (Waltham, MA, USA). FITC Annexin V (640906) was purchased from Biolegend (San Diego, CA, USA). Candesartan (HY-B0205), Bosentan (HY-A0013), Imatinib (HY-15463), BMS-777607 (HY-12076), bemcenti-nib (HY-15150), PD98059 (HY-12028) and PF573228 (HY-10461) were obtained from MedChemExpress (Monmouth Junction, NJ, USA). U46619 (16450) was supplied from Cayman Chemical (Ann Arbor, MI, USA). Murine PDGF-BB (315-18-50) was purchased from Peprotech (Rocky Hill, NJ, USA). UNC2250 (S7342) and ONO-7475 (S8933) were purchased from selleckchem (Houston, TX, USA). KRCT-6j was supplied from Korea Research Institute of Chemical Technology (Daejeon, Republic of Korea). Verteporfin (SML0534) and LY294002 (L9908) were purchased from Sigma-Aldrich (Saint Louis, MO, USA). Rat serum (S17110) was purchased from R&D Systems (Minneapolis, MN, USA). Phophatidylcholine (PC), choles-terol (CH), and phosphatidylserine (PS) were purchased from Avanti Polar Lipids (Alabaster, AL, USA).

csEV isolation, quantification, and characterization
csEVs was isolated from bovine (Invitrogen), porcine (Invitrogen) or rat (R&D systems) serum. Human serum was obtained from healthy non-smoking volunteers. The procedure was approved by Institutional Review Board (IRB) (SNU 19-02-040) in Seoul National University. Serum was serially centrifuged at $300 \times g$ for 10 min, $2500 \times g$ for 20 min, $10,000 \times g$ for 30 min to eliminate cell debris and vesicles larger than sEV. The supernatant was filtered through 0.2 μm filter membrane. The obtained supernatant was diluted with DPBS (1:1) and ultracentrifuged at $120,000 \times g$ for 90 min (Optima XE-100 with SW 32Ti rotor, Beckman Coulter). After the supernatant was discarded, the resident pellet was pipetted in DPBS and subjected to ultracentrifuge at $120,000 \times g$ for 90 min to obtain pure sEV. The csEV pellet was solubilized in DPBS and filtered using 0.2 μm filter. The volume and numerical distribution of the csEV were decided by NanoSight LM10 (Malvern Panalytical,

csEVs promote proliferation and migration of VSMCs
YJ Lee et al.

986

Malvern, UK) and ELSZ-1000 (Photal Otsuka Electronics, Osaka, Japan). csEV were stored at −70 °C and used within 1 month.

Transmission electron microscopy

Sampling of csEV for transmission electron microscopy was performed as previously described [14]. Briefly, isolated csEV was fixed with 4% paraformaldehyde and a diluted solution of csEV was dried on formvar-carbon-coated copper grids for 20 min. After washing with PBS, the grid was post-fixed with 1% glutaraldehyde for 5 min and washed 7–8 times again with distilled water. csEVs were negatively stained with 2% aqueous uranyl acetate for 5 min, dehydrated and completely dried. Further, grids were post-fixed by 1% glutaraldehyde for 5 min followed by rinsing in distilled water (7 times, for 3 min). Enhancing of grids was performed using silver enhancement solution (0.1% silver nitrate, 1% hydroquinone in 0.2 M citrate buffer) for 5 min, followed by rinsing in deionized water. Finally, grids were negatively stained with 2% aqueous uranyl acetate for 5 min and air-dried. The sample images were obtained using transmission electron microscope (LIBRA 120, Carl Zeiss, Oberkochen, Germany).

Preparation of negative charged liposomes

The thin lipid film hydration and extrusion technique with slight modification was used for preparing the negatively charged liposomes as previously described [14].

Western blot analysis

Cell was lysed with sample buffer (10 mM Tris, 100 mM NaCl, 1 mM EGTA, 10% glycerol, 1% TritonX-100 and 30 mM sodium pyrophosphate). Protein samples were separated using sodium dodecylsulfate-polyacrylamide gel electrophoresis (SDS-PAGE) and then transferred to nitrocellulose membranes (GE healthcare, Madison, WI, USA). The membranes were blocked for 1 h in 5% skim milk, and then incubated with primary antibodies at 4 °C overnight. After incubation in secondary antibodies conjugated with horseradish peroxidase antibodies (Cell Signaling Technology, Beverly, MA, USA) for 2 h, protein expression was detected using the Immobilon Western Chemiluminescent HRP Substrate (Merck Millipore, Billerica, MA, USA).

RNA preparation and real-time quantitative polymerase chain reaction

Total RNA was isolated using TRIzol (Thermo Fisher Scientific, Waltham, MA, USA). cDNA was reverse transcribed using Maxime RT PreMix kit (iNtRON, Seongnam, Republic of Korea) from the isolated RNA. mRNA level was quantified by qRT-PCR using SYBR Select Master Mix (Applied Biosystems, Foster City, CA, USA) and Bio-Rad CFX Manager™ Software (Bio-Rad, Hercules, CA, USA) following the manufacturer's instructions.

18 S rRNA (forward: 5′-CCATCCAATCGGTAGTAGCG-3′, reverse: 5′- GTAACCCGTTGAACCCCATT-3′)

Axl (forward: 5′-GTGTTCCTGCCCACTCAGAT-3′, reverse: 5′-GCTA GGTCCCGGTGTATGAA-3′),

Ctgf (forward: 5′-CAAGCTGCCCGGGAAAT-3′, reverse: 5′-CGGTC CTTGGGGCTCATCA-3′),

Cyr61 (forward: 5′-GTGCCGCCTGGTGAAAGAGA-3′, reverse: 5′-GC TGCATTTCTTGCCCTTTTTTAG-3′).

Real-time monitoring of cell proliferation and wound-healing assay using IncuCyte®

VSMCs (7×10^3) were seeded in 96-well plate. After overnight incubation, media was changed to serum free media with csEV and the indicated antagonists. The phase confluence of the cells was scanned by IncuCyte® S3 Live Cell Analysis System (Essen Bioscience, MI, USA). For wound-healing assay, 4×10^4 VSMCs were seeded in IncuCyte® ImageLock plates (Essen Bioscience, MI, USA) and incubated until the cell confluency reached about 95%. 96-Well WoundMaker (Essen bioscience, MI, USA) was used to

make wound scratch and then wound closure was scanned by IncuCyte ZOOM Live Cell Analysis System (Essen Bioscience, MI, USA) every 12 h.

Chemotaxis assay

Boyden chamber assay was used to examine migration of VSMCs. For Transwell migration assay, 1×10^4 cells were seeded using media without FBS in the upper chamber (Corning, New York, USA) pre-coated with 1% type 1 collagen (Sigma-Aldrich, MO, USA), and media with csEV and the indicated antagonists were filled in the lower chamber. VSMCs were incubated for 24 h, and the migrated cells were fixed with 4% paraformaldehyde. The fixed cells were stained using 0.1% crystal violet. The migrated cell number was counted manually using microscope (Olympus IX70, Olympus, Tokyo, Japan).

siRNA knockdown

Scrambled siRNA was used as control siRNA. 100 pmol of pre-designed rat Yap siRNA or Jun siRNA (Bioneer, Daejeon, Republic of Korea) was used to knockdown the indicated genes. VSMCs were transfected with siRNAs using Lipofectamine 2000 (Life Technologies, Carlsbad, CA, USA) following the manufacturer's instructions.

Immunocytochemistry

Cells (1×10^5) were seeded above the cover glass in 12-well plate. After overnight incubation, media was changed to serum free media with csEV and the indicated antagonists. The cells were fixed with 4% paraformaldehyde for 20 min and then incubated with 0.1% Triton X-100 for 15 min. The fixed samples were blocked using 10% horse serum at room temperature for 1 h and incubated with primary antibody overnight. After washing with PBS for 3 times, the cells were incubated with fluorophore-conjugated secondary antibody. The cover glasses were mounted with ProLong Gold Antifade Mountant (Life technologies, Carlsbad, CA, USA) on the slide glass. Confocal microscope (Leica TCS SP8 MP, Leica Microsystems, Wetzlar, Germany) was used to obtain fluorescence images.

Statistical analysis

GraphPad PRISM software (GraphPad Software Inc., San Diego, CA, USA) was used for statistical analysis. The data are shown as means ± SD. Unpaired Student's t-test or one-way analysis of variance (ANOVA) followed by the Tukey's test was used to evaluate statistical significance. Results with P-value < 0.05 were considered significant.

RESULTS

csEVs promote proliferation and migration of VSMCs via phosphatidylserine

We isolated csEVs from bovine, porcine, and rat sera by a serial ultracentrifugation method. We mainly used bovine csEVs throughout this study, and verified key data with rat csEV [14]. The same lot number of serum was used to minimize intraspecies variance. To determine whether the csEVs isolated from serum possess typical characteristics of sEVs, we identified their morphology and size. A transmission electron microscopy (TEM) image revealed vesicles of around 100 nm diameter (Fig. 1a). To further verify the size distribution of the isolated csEV, direct light scattering was performed. The size of the particles was smaller than 200 nm, with a mean of 166.9 ± 3.3 nm (Fig. 1b). The csEVs were labeled with a lipophilic fluorescent dye, DiD, to investigate their interaction with VSMCs. A confocal microscopy image after incubation with the DiD-labeled csEVs showed that they had been uptaken by VSMCs (Fig. 1c). Consistent with this result, VSMCs incubated with DiD-labeled csEV exhibited enhanced fluorescence intensity on flow

csEVs promote proliferation and migration of VSMCs
YJ Lee et al.

987
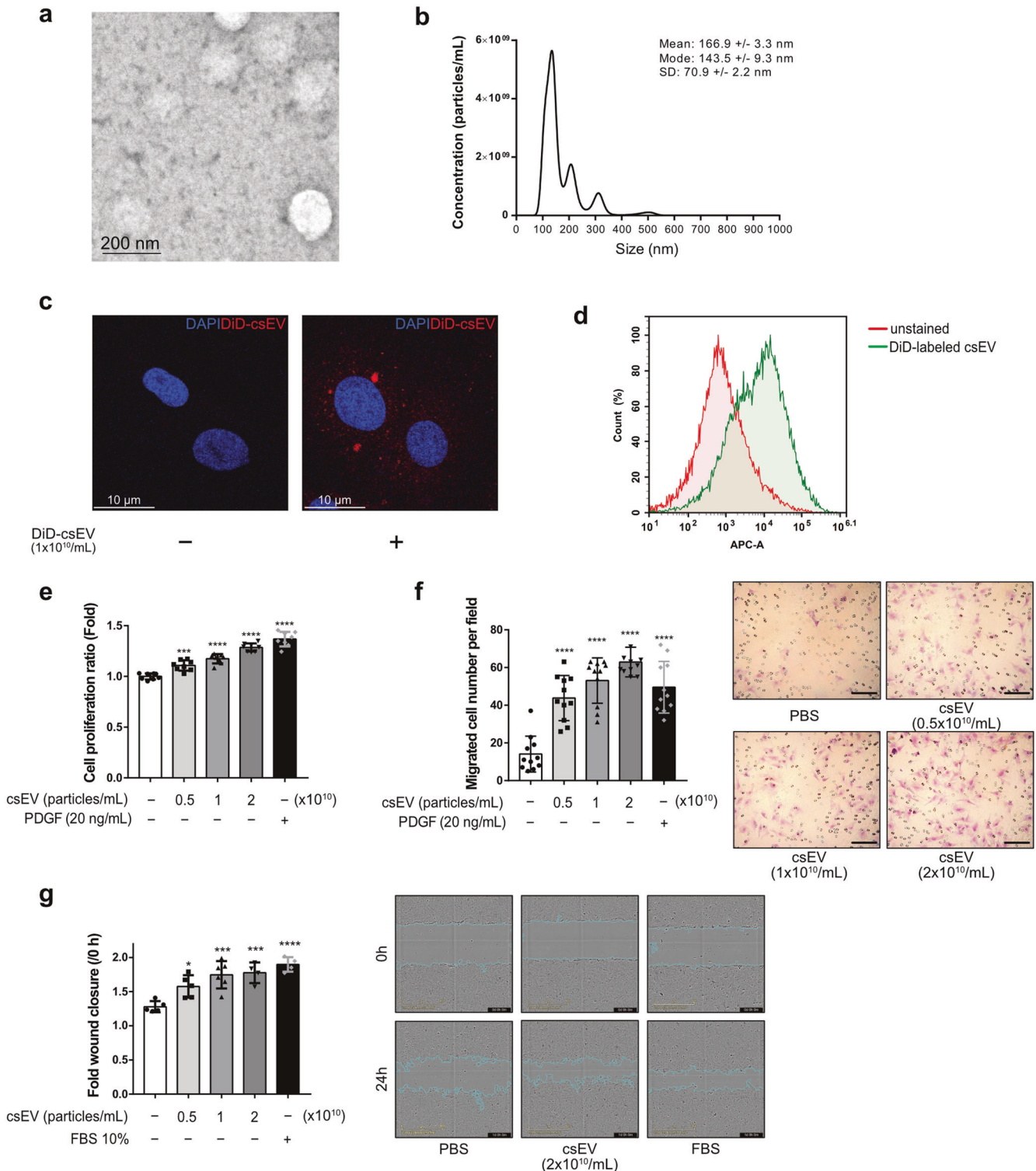
Fig. 1 **csEV-induced proliferation and migration of VSMCs. a** Representative transmission electron microscopy image of csEV (Scale bar, 200 nm). **b** Rat-csEV size distribution was measured using NanoSight. **c** VSMCs were incubated with DiD-labeled csEV for 2 h. Immunofluorescence image of DiD-labeled csEV (red) and their binding to VSMC (blue-DAPI) (Scale bar, 10 μm). **d** Representative flow cytometry result showing VSMCs bound to DiD-labeled csEV. **e** VSMCs were incubated with csEV for 48 h. Cell proliferation was evaluated using IncuCyte S3® system ($n = 8$). **f** VSMC was seeded into the upper chamber of the Transwell system and csEV was added to the lower chamber. Cell migration was quantified 24 h after csEV treatment ($n = 11$). Representative images of migrated cells are shown to the right (Scale bar, 100 μm). **g** A scratch was made through VSMC layer, then cells were incubated with csEV. After 24 h, wound closure was measured by calculating the width of the wound ($n = 4–6$). Microphotographs of the wounded area are shown to the right (Scale bar, 800 μm). Data represent means ± SD. Statistical significance was determined using one-way ANOVA followed by Tukey-Kramer multiple-comparisons test. $*P < 0.05$; $***P < 0.001$; $****P < 0.0001$, significant as compared to vehicle-treated group or indicated group.

csEVs promote proliferation and migration of VSMCs
YJ Lee et al.

988

cytometry, which results also are indicative of direct interaction between csEV and VSMC (Fig. 1d).

To confirm whether csEV induce proliferation and migration of VSMC, VSMCs were incubated with csEV according to predetermined time points. We found that the csEVs enhanced not only the proliferation but also the migration and wound-healing of VSMCs compared to the vehicle (Dulbecco's Phosphate-Buffered Saline, DPBS) (Fig. 1e–g): 1.29-fold (2×10^{10}/mL csEV) vs 1.37-fold (Platelet derived growth factor, PDGF) relative to vehicle, 4.46-fold (2×10^{10}/mL csEV) vs 3.52-fold (PDGF) relative to vehicle, and 1.38-fold (csEV) vs 1.48-fold (FBS) relative to vehicle, respectively, even at the minimum csEV concentration of 0.5×10^{10} per mL. The stimulatory effects of csEV on the proliferation and migration of VSMCs were increased in a concentration-dependent manner. csEVs isolated from porcine and rat serum showed the same effects on the VSMCs and bovine csEVs also did, on the mouse VSMCs (Supplementary Fig. S1).

In our previous study, exposure of PS in csEVs was shown to be critical to the migratory effect of csEV on cancer cells [14]. The membrane-lipid composition of csEVs secreted by diverse cell types differs from that of parent cells in their enrichment factors, containing two to three times more PS compared to parent cells [17]. In the present study, to measure the PS exposure of the isolated csEVs, we analyzed their binding ability to Annexin V, which is widely used to label PS in apoptotic cells or PS-rich vesicles. Artificial liposomes composed of phosphatidyl choline (PC) and cholesterol (CH) (2:1) (PC liposomes) or PC, CH, and PS (1:1:1) (PS liposomes) were used as the control. The fluorescent intensity of Annexin V-FITC was higher in the isolated csEV than in PC liposomes or even PS liposomes, indicating that PS is abundantly distributed in the outer membrane of csEVs (Supplementary Fig. S2).

To unravel the involvement of membrane PS in the csEV-induced VSMC proliferation and migration, VSMCs were subjected to artificial liposomes. Treatment with PS liposomes was found to slightly but significantly enhance the proliferation and migration of VSMCs compared with the vehicle or PC liposomes (Fig. 2a, b). To further verify the effect of PS, PS on the surface of the csEVs was blocked with Annexin V [18, 19]. Pre-incubation of the csEVs with Annexin V partially reversed the proliferation rate increased by csEV (Fig. 2c). In addition, a Transwell migration assay demonstrated that the migration of VSMCs induced by csEVs was significantly inhibited by pre-incubation with Annexin V (Fig. 2d). To exclude the effects of cargo proteins in csEVs, we performed proliferation assays with several antagonists targeting receptors for representative VSMC mitogens, PDGFβ, angiotensin II, endothelin, and thromboxane A2 (Supplementary Fig. S3). None of the antagonists significantly altered the csEV-induced proliferation of VSMCs. Taken together, our data indicate that membrane PS of csEVs plays as a crucial factor to stimulate transformation into proliferative and migratory phenotypes of VSMC.

We further investigated whether csEVs or PS liposomes aggravate neointimal hyperplasia in vivo. For the purposes of a perturbed-blood-flow-induced neointimal hyperplasia model, we performed total ligation of the right carotid artery of Sprague Dawley rats. After the ligation injury, pluronic F-127 hydrogel preloaded with either csEV, PS liposome or vehicle was applied to the ligation region. Two weeks after the injury, the effect of csEV or PS liposomes on neointima formation was evaluated by H&E staining. The neointima/media ratio of the neointima-formed arteries showed increased neointima area in both the csEV- and PS-liposome-treated groups (Fig. 2e, f). Moreover, the number of Sprague-Dawley rats with detectable neointima was higher in both treated groups compared with the vehicle-treated (control) group: csEV (7/10) 70%, PS liposome (7/9) 77.78%, control (3/9) 33.33% (Fig. 2g). Based on these results, we suggest that csEVs in blood flow aggravate neointima formation via membrane PS upon injury.

csEV-induced proliferation and migration of VSMCs is dependent on AXL and MerTK

We examined whether the effects of csEVs on VSMCs are dependent on TAM receptors. Both protein ligands and PS lipid moiety are required for optimal activation of TAM receptors. Therefore, we investigated the existence of bridging ligands under our experimental conditions. GAS6 was found in the conditioned medium of VSMC [20], and the TEM images of csEVs revealed the presence of PROS1 in the membrane [14]. We also verified the existence of GAS6 and PROS1 in an csEV-rich fraction obtained by density gradient ultracentrifugation (Supplementary Fig. S4). We examined the expression levels of TAM receptors in VSMCs compared with those in HCT116, human colon cancer cells highly expressing all three TAM receptors, and LNCaP-SL, a human prostate cancer cell line highly expressing TYRO3 [14]. Compared with the two cancer cell lines, the VSMCs showed higher expression of AXL, while MerTK and TYRO3 expressions were relatively lower (Fig. 3a). Both MerTK and AXL were phosphorylated by csEV treatment within 30 min, whereas no phosphorylation of TYRO3 was observed, presumably due to the low expression relative to AXL and MerTK (Fig. 3b). To assess whether activation of TAM receptors is required for csEV-induced proliferation and migration of VSMCs, the effects of TAM receptor inhibitors were assessed. The inhibitors were used at a concentration below the level at which VSMC viability change is detected. BMS777607, a pan-TAM inhibitor, significantly inhibited all of the effects of csEVs. To further investigate the three TAM receptors' mediation of the effects of csEVs, selective inhibitors targeting AXL, MerTK and TYRO3 were used. Bemcentinib (AXL inhibitor) and UNC2250 (MerTK inhibitor) significantly reduced the csEV-stimulated proliferation and migration of VSMCs (Fig. 3c–e). However, KRCT-6j, a selective TYRO3 inhibitor, did not reverse any of the effects of csEVs (Fig. 3c–e). Our results demonstrate that AXL and MerTK actively participate in the interaction between csEVs and VSMCs.

Akt, ERK and FAK signaling pathways are activated by csEVs to stimulate proliferation and migration of VSMCs

To further explore the downstream signaling of AXL/MerTK, we examined the Akt/mTOR/S6K and ERK pathways. The Akt/mTOR/S6K signaling pathway has been widely reported to induce cell survival, proliferation and migration under all three TAM receptors in numerous cell types [21]. AXL and MerTK, as stimulated by GAS6, an endogenous ligand for TAM receptors, are also coupled with the ERK pathway responsible for the increased proliferation and survival of NIH3T3 fibroblasts [22]. We found that both Akt and ERK were activated by csEV in a concentration-dependent manner (Fig. 4a, b). Akt was maximally phosphorylated at 1 h and then de-phosphorylated 6 h after csEV exposure (Fig. 4c), while csEV phosphorylated ERK faster, with the peak time of 15 min (Fig. 4d). To verify whether the activation of Akt and ERK is dependent on either AXL or MerTK, VSMCs were pretreated with bemcentinib (AXL-selective inhibitor) or UNC2250 (MerTK-selective inhibitor) prior to csEV exposure. Both Akt and ERK signaling pathways were indeed under the influence of AXL and MerTK, as evidenced by the phosphorylation inhibition by the RTK inhibitors (Fig. 4e–h). Moreover, the csEV-induced proliferation and migration of VSMCs were markedly reduced by LY294002 (PI3-kinase inhibitor) or PD98059 (ERK inhibitor) pretreatment (Fig. 4i-l). These results indicate that the PI3-kinase/Akt and ERK pathways are downstream targets of AXL and MerTK, and function as key players in csEV-mediated proliferation and migration of VSMCs.

Focal adhesion kinase (FAK) serves as a central mediator of cell movement, recruiting other adaptor proteins such as paxillin to the focal adhesion site [23]. In non-small cell lung cancer cells, reportedly, FAK acted downstream of AXL and MerTK to mediate migration and invasion [24]. In the present study, csEV increased Y397 autophosphorylation of FAK and phosphorylation of paxillin
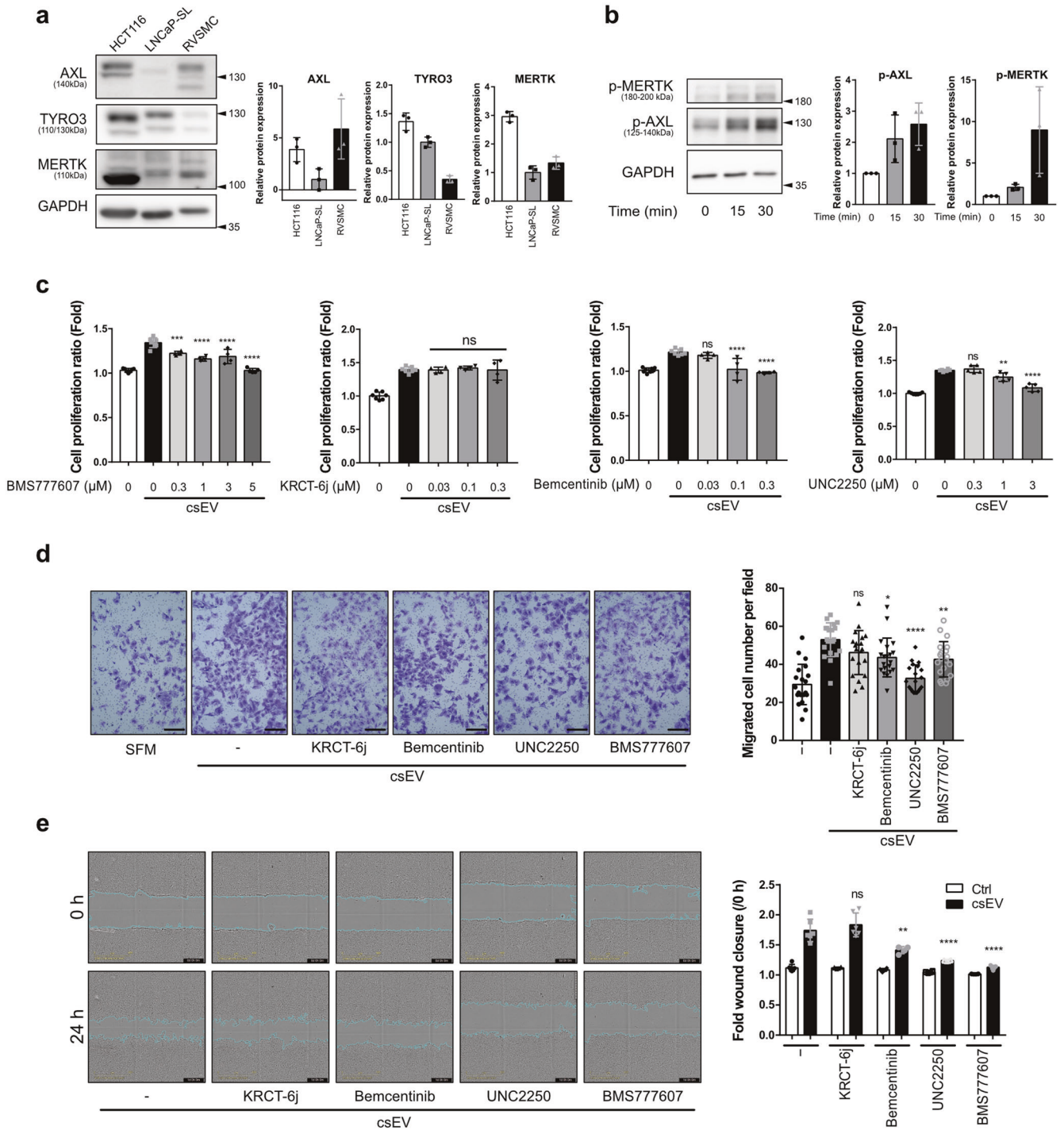
csEVs promote proliferation and migration of VSMCs
YJ Lee et al.

989
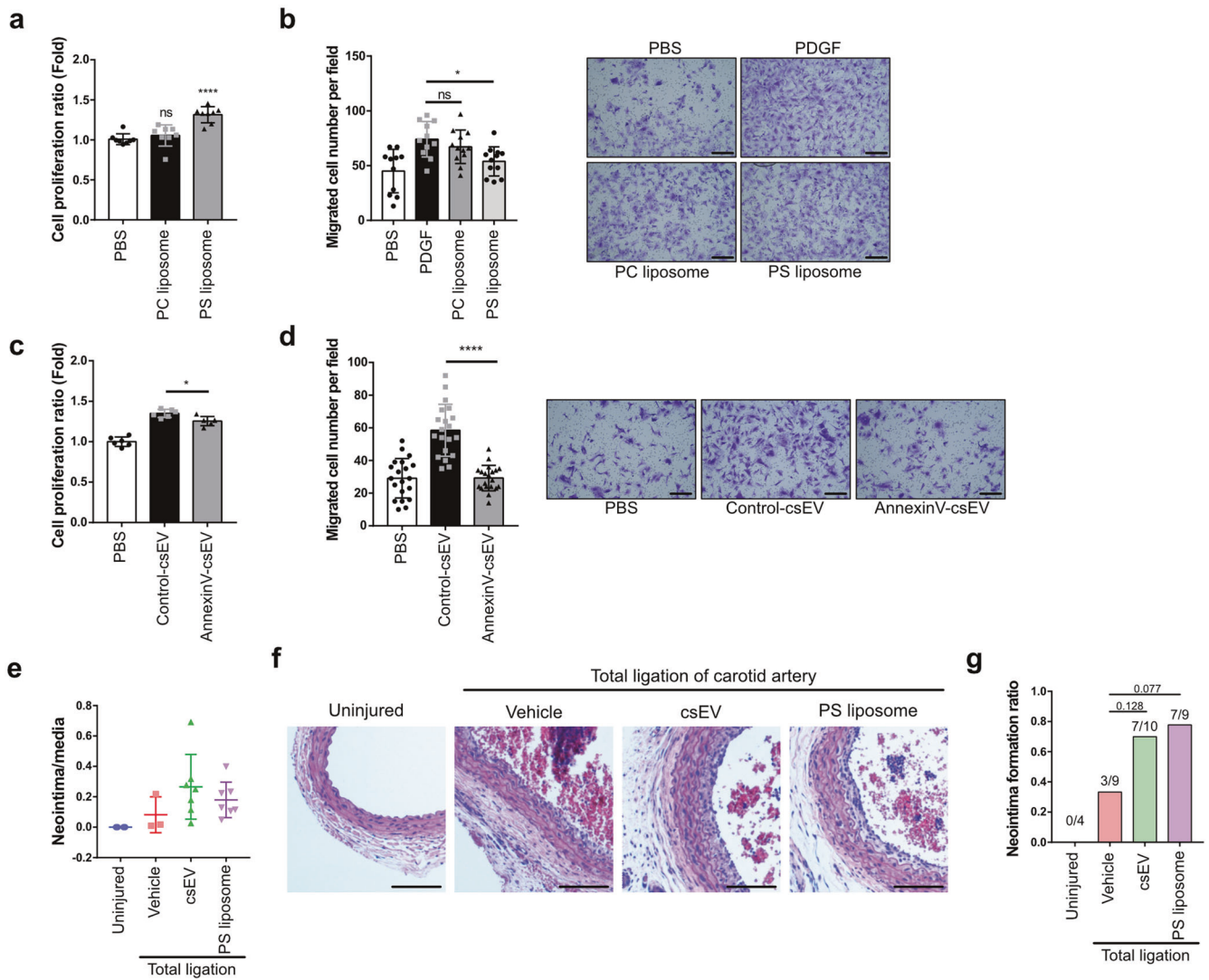
Fig. 2 Involvement of phosphatidylserine membrane structure in csEV-VSMC interaction. a VSMCs were incubated with artificial liposomes (PC liposomes or PS liposomes). Effects of the artificial liposomes on proliferation of VSMC were measured using IncuCyte® S3 system ($n = 8$). **b** Cell migration was monitored after incubation with artificial liposomes for 24 h ($n = 11$; Scale bar, 200 μm). **c** csEV were pre-incubated with Annexin V before addition to VSMCs. The proliferation ratio at 48 h ($n = 6$) and (**d**) migrated cell number at 24 h after exposure of csEV were assessed ($n = 20$; Scale bar, 200 μm). **e** H&E staining of ligated artery in each group 2 weeks after total ligation of right carotid arteries. The relative area ratios of neointima to media were calculated ($n = 4, 3, 7, 7$ respectively) and (**f**) the representative images of the cross section are shown. **g** The ratio of neointimal formation was represented, statistical significance was determined using Fisher's exact test and represented P-value was calculated compared to vehicle-treated group ($n = 4, 9, 10, 9$ respectively; Scale bar, 250 μm). Data represent means ± SD. Statistical significance was determined using one-way ANOVA followed by Tukey-Kramer multiple-comparisons test. *$P < 0.05$; **** $P < 0.0001$, significant as compared to vehicle-treated group or indicated group.

from 15 min to 180 min in VSMCs (Fig. 5a, b). The enhanced phosphorylation of paxillin was further detected by immunocytochemistry at the focal adhesion site of VSMCs 1 h after csEV exposure (Fig. 5c). PF573228, a selective FAK inhibitor, effectively reversed the activation of FAK (Fig. 5c), and csEV-induced migration of VSMC was markedly reduced by PF573228 treatment (Fig. 5d). Moreover, pretreatment of VSMC with either bemcentinib or UNC2250 partially inhibited activation of FAK induced by csEV, demonstrating that FAK acts as a downstream target for AXL- or MerTK-mediated VSMC migration (Fig. 5e, f). However, FAK inhibition by PF583228 did not affect the csEV-induced proliferation of VSMCs (Supplementary Fig. S5).

AXL expression is elevated by csEV via YAP activation
In the injured vascular wall, the level of AXL is increased to stimulate the proliferation and migration of VSMCs [16]. However,

the pathophysiological mediator of AXL induction in the vascular system has yet to be elucidated. csEV treatment for 360 min significantly elevated both AXL protein and transcript levels in VSMCs, whereas the MerTK protein expression was not changed (Fig. 6a, b). We then tried to assess the essential transcription factor(s) for stimulation of *Axl* gene transcription in csEV-treated VSMCs. Reportedly, YAP and c-JUN are involved in transcriptional activation of the *Axl* gene in several cancer cell types, including lung cancer [25] and leukemia cells [26]. We found that both YAP and c-JUN were activated by csEV in VSMCs (Fig. 6c and Supplementary Fig. S6). After 1 h incubation with csEV, YAP was translocated to the nucleus (Fig. 6d). The mRNA levels of *Ctgf* and *Cyr61*, the representative target genes of YAP activation, also were elevated by csEV (Fig. 6e). We next performed siRNA knockdown of *Jun* or *Yap* in order to verify that c-JUN or YAP affects AXL induction by csEV. In the results, csEV-enhanced AXL expression

csEVs promote proliferation and migration of VSMCs
YJ Lee et al.

990

Fig. 3 AXL/MerTK-dependent proliferation and migration of VSMC. a Immunoblottings for TAM receptors (TYRO3/AXL/MerTK) in VSMCs. Total cell lysates from HCT116 cells were used as positive control for TYRO3/AXL/MerTK and LNCaP-SL cell lysates were used as positive control for TYRO3 ($n = 3$). **b** VSMCs were incubated with csEV for the indicated time points. Phosphorylation of AXL and MerTK were detected by immunoblottings ($n = 3$). **c** VSMCs were treated with BSM777607 (pan-TAM inhibitor), KRCT-6j (TYRO3 inhibitor), bemcentinib (AXL inhibitor) or UNC2250 (MerTK inhibitor) prior to incubation with csEV. Proliferation ratio was measured 48 h after csEV exposure ($n = 4$–8) and (**d**) the number of migrated VSMCs was quantified at 24 h (3 μM BMS777607, 0.3 μM KRCT-6j, 0.3 μM bemcentinib, 1 μM UNC2250) ($n = 20$; Scale bar, 200 μm). SFM serum free media. **e** Scratched layer of VSMCs was treated with TAM inhibitors prior to incubation with PBS (vehicle) or csEV. Wound closure was measured by calculating the wound closure at 24 h ($n = 6$; Scale bar, 800 μm). Data represent means ± SD. Statistical significance was determined using one-way ANOVA followed by Tukey-Kramer multiple-comparisons test. **$P < 0.01$; ***$P < 0.001$; ****$P < 0.0001$, significant as compared to vehicle-treated group or csEV-treated group.

was reversed by *Yap* siRNA, but not by *Jun* siRNA, indicating that YAP acts as the main regulator of *Axl* gene transcription in VSMCs (Fig. 6f, g, and Supplementary Fig. S6). We also found that the YAP/TEAD inhibitor (Verteporfin) markedly inhibited AXL

expression increase, which further corroborates the key role of YAP in csEV-mediated AXL gene upregulation (Fig. 6h, i).

Recent studies have demonstrated that FAK regulates the non-canonical YAP pathway with phosphorylating tyrosine 357 and

csEVs promote proliferation and migration of VSMCs
YJ Lee et al.

991
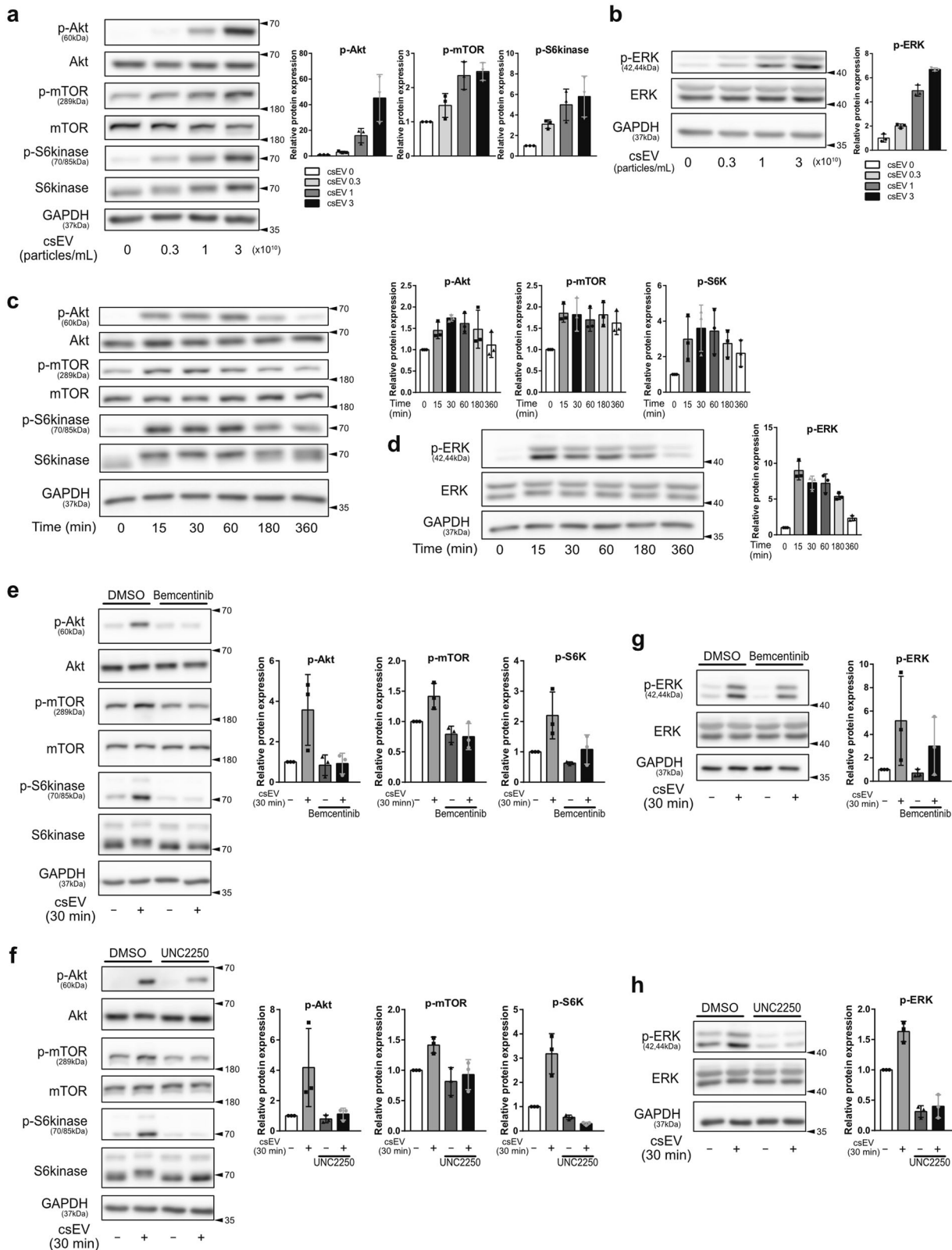
Fig. 4 (Continued).

promotes the nuclear localization of YAP [27, 28]. Because FAK is activated by csEV exposure (Fig. 5a, b), we investigated whether YAP is a downstream target of FAK. In VSMCs, PF573228 significantly inhibited csEV-induced phosphorylation of Y357 YAP (Fig. 7a). Immunocytochemistry confirmed that

PF573228 hindered nuclear translocation of YAP and mitigated the mRNA increase in *Ctgf* or *Cyr61* in csEV-exposed VSMCs (Fig. 7b, c). Accordingly, pretreatment of VSMCs with PF573228 significantly inhibited AXL induction by csEVs (Fig. 7d, e). The data support the notion that FAK, as a key regulator of YAP,

csEVs promote proliferation and migration of VSMCs
YJ Lee et al.

992
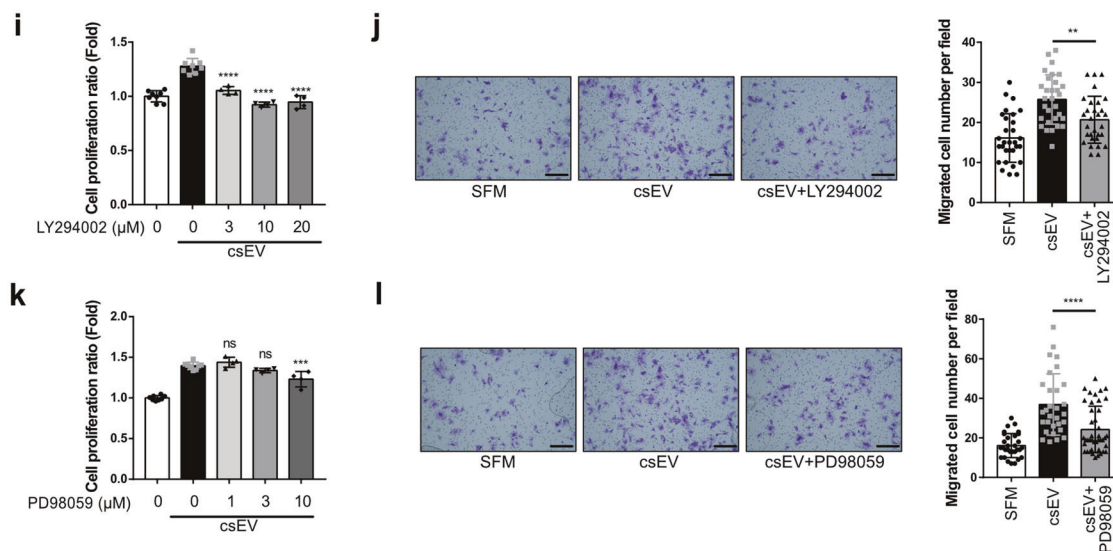
Fig. 4   Role of csEV-induced Akt/mTOR/S6K and ERK activation in the proliferation and migration of VSMC. a, **b** Concentration- and (**c**, **d**) time-dependent activation of Akt/mTOR/S6K and ERK in csEV-treated VSMCs ($n = 3$). Protein expression of p-Akt, Akt, p-mTOR, mTOR, p-S6K and S6K in VSMCs was determined by immunoblottings after incubation with (**e**) bemcentinib or (**f**) UNC2250 in the presence of csEV ($n = 3$). Expression of p-ERK and ERK in VSMCs was measured by immunoblottings after incubation with (**g**) bemcentinib or (**h**) UNC2250 in the presence of csEV ($n = 3$). Effects of LY294002 (10 μM) on (**i**) proliferation ($n = 4$–8) and (**j**) migration of VSMCs treated with csEV ($n = 30$). Representative images of migrated cells were shown to the left (Scale bar, 200 μm). Effects of PD98059 (10 μM) on (**k**) proliferation ($n = 4$–8) and (**l**) migration of VSMCs treated with csEV ($n = 30$–42; Scale bar, 200 μm). Data represent means ± SD. Statistical significance was determined using one-way ANOVA followed by Tukey-Kramer multiple-comparisons test. **$P < 0.01$; ***$P < 0.001$; ****$P < 0.0001$, significant as compared to vehicle-treated group or csEV-treated group.

is actively involved in enhancing *Axl* gene transcription by csEVs. In summary, csEVs activate FAK to phosphorylate YAP, which elevates AXL expression and mediates the possibly positive feedback effects of csEVs in VSMCs.

**Dual inhibition of AXL and MerTK effectively blocks csEV effects on VSMC**

We demonstrated that csEVs promote the proliferation and migration of VSMCs via AXL and MerTK, and that these two receptors share downstream signaling pathways. Hence, we evaluated whether the dual inhibition of AXL and MerTK completely blocked the effects of the csEVs on the VSMCs. Dual inhibition was accomplished by concurrent treatment of bemcentinib and UNC2250 or by using ONO-7475, an inhibitor with dual selectivity on AXL/MerTK. ONO-7475 almost completely abolished the activation of the downstream signaling pathways of csEVs (Fig. 8a). The phosphorylations of Akt and its downstream targets mTOR and S6K were almost completely suppressed (Fig. 8a) relative to the partial inhibition achieved by selective inhibition of either receptor (Fig. 4c, d). The activities of the ERK and FAK/YAP pathways also were inhibited by ONO-7475 (Fig. 8a). Moreover, VSMC proliferation and migration induced by csEVs were markedly reduced by cotreatment with bemcentinib and UNC2250, dual AXL/MerTK inhibition (Fig. 8b, c) or ONO-7475 (Fig. 8d, e). Next, we further tested the effects of dual AXL/MerTK inhibition on csEV-induced AXL induction. The csEV-stimulated mRNA increase of *Axl* was completely reversed by dual AXL/MerTK inhibition (Fig. 8h) versus the partial inhibition by bemcentinib or UNC2250 (Fig. 8f, g). Unfortunately, TAM receptor knockout mice were reported to develop various systemic autoimmune diseases [29, 30]. To investigate AXL/MerTK inhibition in vessels, we used ex vivo aorta injury model. The isolated mouse aortas were injured by physical insertion of 24-gauge needle, and the aorta sections were incubated with or without ONO-7475 for 5 days. The medial thickness of ONO-7475 treated aortas showed decreased medial area (Fig. 8i). These results suggest that dual inhibition of AXL/MerTK more

effectively hinders csEV-mediated proliferation and migration of VSMCs.

DISCUSSION

Herein, we have demonstrated that csEV promotes the proliferation and migration of VSMCs by activating AXL/MerTK. Recent studies have revealed that sEV from different origins (e.g., macrophages, endothelial cells) exerted similar effects on VSMCs, promoting migratory and/or proliferative phenotypes [9, 10, 31]. We likewise observed that csEV isolated from three different species evoked the same effects on VSMCs, and representative mitogens to VSMC, PDGF, endothelin and thromboxane A2 were not involved in csEV-mediated VSMC proliferation or migration. Therefore, we assumed that csEV, as the most abundant sEVs in the blood circulation, would participate in the pathogenic transition of VSMCs, and presumably not through cargo proteins. Given that the number of circulating EVs is significantly elevated in patients with chronic vascular diseases such as atherosclerosis and restenosis [7], the impact of csEVs on the vascular system can be intensified. A very recent study showed that sEVs isolated from rat plasma promote the proliferation and migration of VSMCs [32]. However, the researchers did not elucidate the mechanisms underlying the interaction between csEVs and VSMCs.

In our previous study, we demonstrated that negatively charged csEVs promote the migration of cancer cells [14]. Among the candidates for the negative charge, PS was revealed to be responsible for the increased migration of cancer cells [14]. Based on this result, we created artificial liposomes in the same way and treated them to VSMCs. The PS liposomes promoted the proliferation and migration of VSMCs, like csEVs, and these effects were reversed by the PS-binding inhibitor, Annexin V. Also in a neointimal hyperplasia animal model, we showed that csEV or PS liposome treatment to the injured artery tends to increase not only the neointima formation ratio but also the intima/media ratio in the arteries containing the neointima region (Fig. 2). As PS-

csEVs promote proliferation and migration of VSMCs
YJ Lee et al.

993
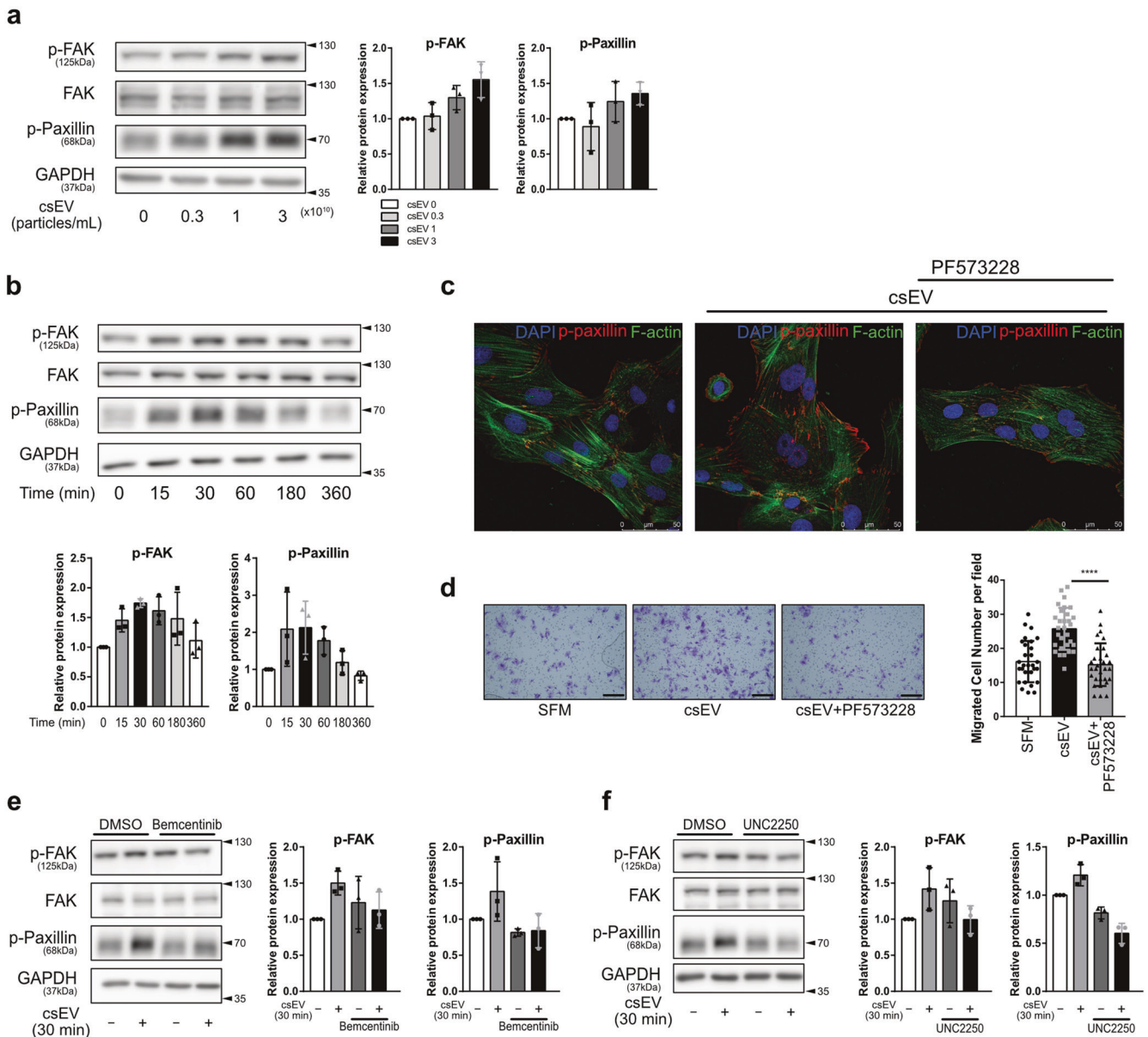
Fig. 5 Involvement of FAK activation in csEV-induced VSMC migration. a Concentration- and (**b**) time-dependent activation of FAK and paxillin by csEV in VSMCs. FAK activation was determined by immunoblottings using phosphorylation (Tyr397)-specific FAK antibody ($n = 3$). **c** Immunofluorescence images of p-paxillin in VSMCs. VSMCs were treated with csEV in the presence or absence of 3 μM PF573228. After 1 h incubation, immunocytochemical stainings of DAPI (blue), p-paxillin (red) and F-actin (green) were performed (Scale bar, 50 μm). **d** Effect of PF573228 on csEV-induced VSMC migration. Representative images of migrated cells are shown to the left ($n = 30$; Scale bar, 200 μm). The phosphorylation of FAK and paxillin was assessed by immunoblottings in VSMCs incubated with csEV in the presence of (**e**) bemcentinib or (**f**) UNC2250 ($n = 3$). Data represent means± SD. Statistical significance was determined using one-way ANOVA followed by Tukey-Kramer multiple-comparisons test. ****$P < 0.0001$; ns, not significant, significant as compared with indicated group.

sensing receptors, the roles of the TAM receptor family (TYRO3, AXL, and MerTK) have been investigated in vascular diseases, AXL being especially well known as a receptor that regulates the proliferation and migration of VSMCs [33]. The interaction of AXL with GAS6, a circulating ligand for TAM receptors, is increased in the course of vascular damage infliction and promotes the proliferation and migration of VSMCs [16, 34]. However, the functional roles of PS and other TAM receptors remain unelucidated. The role of MerTK in vascular diseases has been investigated mainly in phagocytic immune cells; it has not yet been clarified for VSMCs [33]. Here in the present study, we verified that coordinated activation of AXL and MerTK is required for sustained activation of PI3-kinase/Akt/mTOR and Ras/Raf/ERK

signaling pathways by csEVs, which is eventually critical to VSMC proliferation and migration.

The PI3-kinase/Akt/mTOR and Ras/Raf/ERK signaling pathways are representative downstream kinases of AXL [35, 36]. It has been proposed that MerTK also activates Akt in several cancer cells [37], though MerTK signaling in VSMCs has not been fully identified. Our results showed that both signaling pathways were activated by csEV via the concomitant stimulation of AXL and MerTK. In fact, phosphorylation of FAK, a well-known mediator of cell movement via cytoskeleton rearrangement in VSMCs, has been reported to be increased by vascular damage or stimuli with multiple growth factors [38]. We demonstrated that FAK activation is also related to enhanced migration of VSMCs after csEV binding to AXL and

csEVs promote proliferation and migration of VSMCs
YJ Lee et al.

994
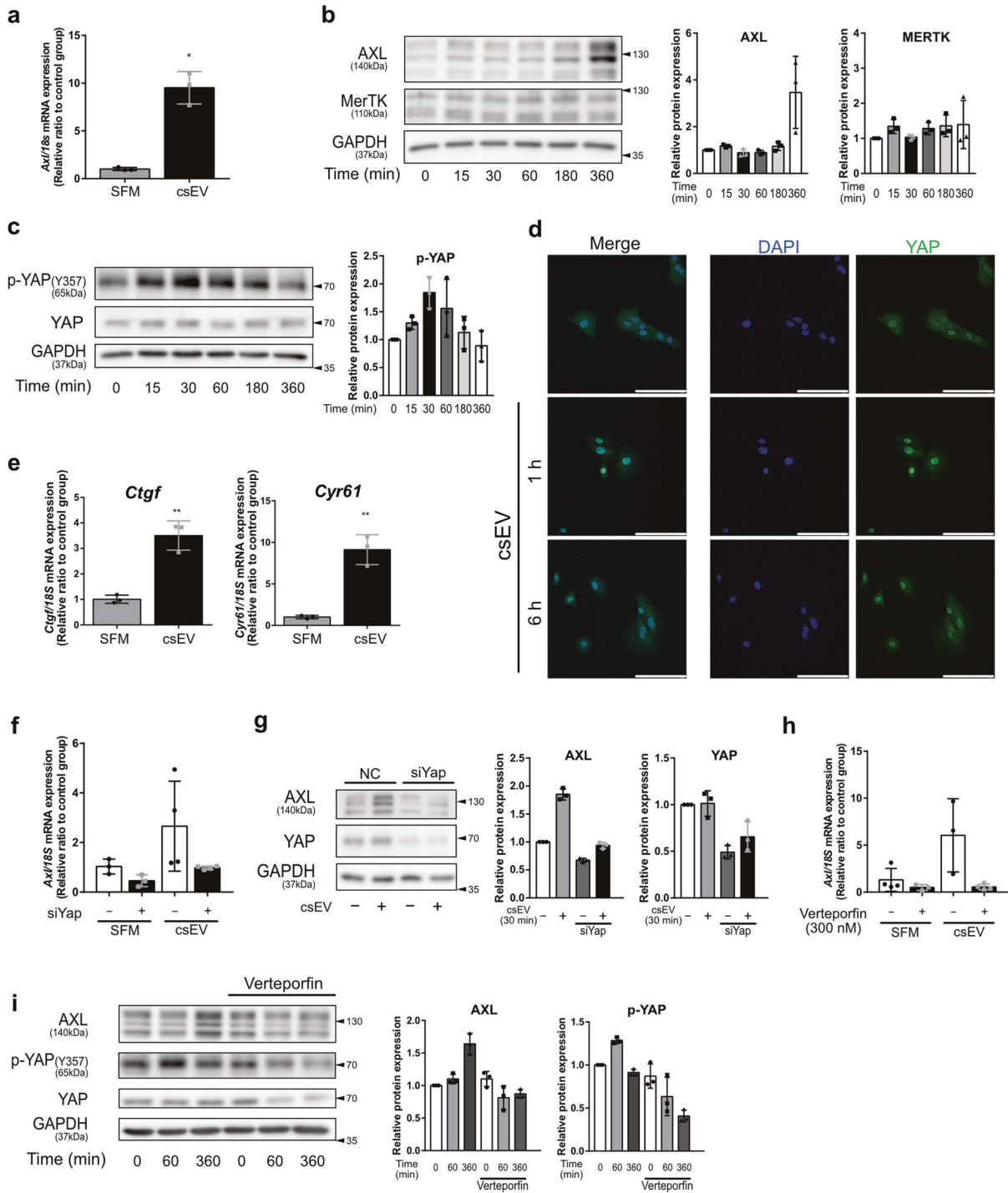
Fig. 6 YAP-dependent AXL upregulation in csEV-treated VSMC. a *Axl* mRNA level. VSMCs were exposed to csEV for 6 h, and total RNA samples were subjected to real-time qPCR (*n* = 4). **b** Protein expression of AXL and MerTK. VSMCs were exposed to csEV for the indicated time points, and total cell lysates were subjected to immunoblottings (*n* = 3). **c** Time-dependent YAP (Y357) phosphorylation by csEV (*n* = 3). **d** Immunofluorescence images of YAP. VSMCs were incubated with vehicle or csEV for 0, 1 and 6 h, and immunocytochemical stainings of DAPI (blue), YAP (green) were performed (Scale bar, 100 μm). **e** mRNA levels of *Ctgf* and *Cyr61* in VSMCs incubated with csEV for 6 h (*n* = 3–4). Effect of (**f, g**) *Yap* siRNA or (**h, i**) verteporfin (YAP-TEAD inhibitor, 300 nM) on (**f, h**) the mRNA levels of *Axl* (*n* = 3–4) and (**g, i**) protein expression of AXL and p-YAP (*n* = 3). VSMCs were incubated with vehicle or csEV for 6 h, and *Axl* mRNA levels were detected using real-time qPCR. SFM; Serum free media, NC; Negative control. Data represent means ± S.D. Statistical significance was determined using unpaired Student's *t*-test. *$P < 0.05$; **$P < 0.01$; ns, not significant, significant as compared to vehicle-treated group or indicated group.

MerTK. While both the PI3K and Ras signaling axes are involved in the proliferation and migration of VSMCs as downstream targets of csEV-activated AXL and MerTK, the FAK signal promotes only VSMC migration, and seems not to be related to proliferation. This finding is in contrast to that of a previous study, which linked FAK activation to proliferation signals [39].

It has been suggested that the expression of AXL increases in the neointima region formed in vascular diseases. Although a

csEVs promote proliferation and migration of VSMCs
YJ Lee et al.

995
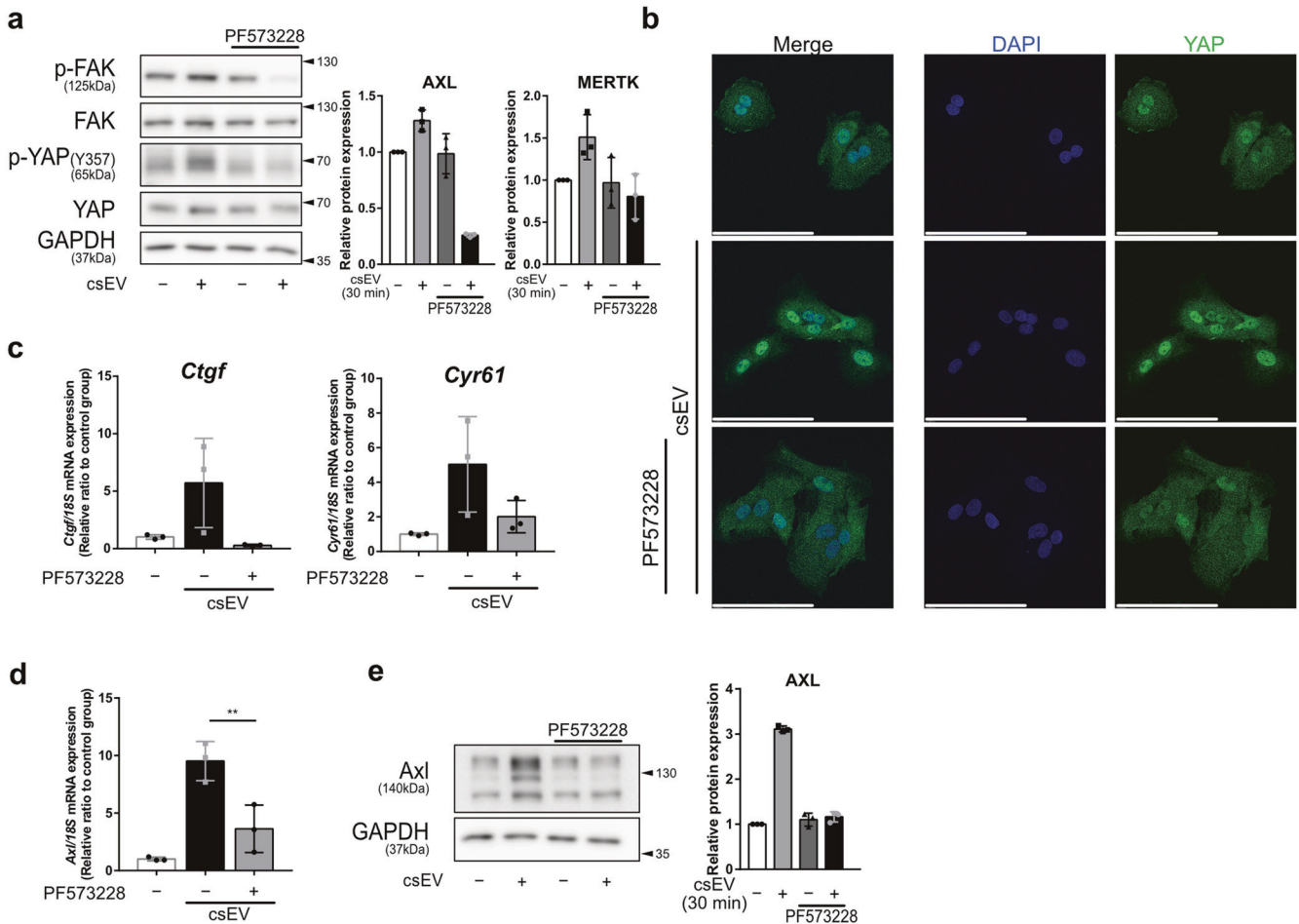
Fig. 7 **Role of FAK in csEV-mediated YAP activation. a** Immunoblottings for p-FAK, FAK, p-YAP and YAP. VSMCs were treated with csEV in the presence or absence of PF573228 ($n = 3$). **b** YAP immunofluorescence images in VSMCs. VSMCs were incubated with PF573228 and csEV for 1 or 6 h, and immunocytochemical staining for DAPI (blue) and YAP (green) was performed (Scale bar, 100 µm). Effect of PF573228 on csEV-induced mRNA expression of (**c**) *Ctgf*, *Cyr61* and (**d**) *Axl*. VSMCs were incubated with csEV for 6 h in the presence or absence of PF573228, and mRNA levels were quantified using real-time qPCR ($n = 3$–4). **e** Effects of PF573228 on csEV-induced protein expression of AXL in VSMCs ($n = 3$). Data represent means ± S.D. Statistical significance was determined using one-way ANOVA followed by Tukey-Kramer multiple-comparisons test. **$P < 0.01$; ns, not significant, significant as compared to csEV-treated group or indicated group.

previous study showed that AXL expression in the vascular wall is increased by angiotensin II and thrombin [40], the exact mechanism has not been identified. Here, we found that AXL expression was enhanced by csEV exposure in VSMCs. Because csEVs elevated both the protein and mRNA levels of AXL, csEV-induced AXL upregulation seems to be related to transcriptional regulation of the gene. Recent studies using cancer cells have shown that crosstalk between YAP and AXL is important to chemotherapy resistance [25, 41]. Moreover, YAP-mediated transcriptional activity is amplified by AXL via Hippo-independent Tyr391/Tyr407 phosphorylation, and conversely, *Axl* gene transcription is stimulated by YAP [41, 42]. Our results showed that csEVs stimulate nuclear translocation of YAP through its receptor binding to AXL and MerTK, and that the activated YAP, in turn, increases the expression of AXL, thus completing a positive feedback loop. In addition, we confirmed that FAK regulates the nuclear translocation of YAP. These findings suggest that csEVs' actions on VSMC could be constantly amplified via the unique YAP/AXL-positive feedback loop.

Among the three TAM receptors, we revealed that MerTK as well as AXL was activated by csEVs in VSMCs. Previous studies have reported that TAM receptors, especially AXL and MerTK,

share an endogenous ligand and the canonical downstream signaling pathways, namely the PI3-kinase/Akt/mTOR/p70S6 kinase and RAS/Raf/ERK pathways, in cancer and immune cells [35, 37]. Hence, if only one of the two TAM receptors on which csEVs act is blocked, the maximal inhibitory effect may not appear, due to the compensatory activation of the other receptor signaling pathway. In fact, when the selective inhibitor solely targeting AXL or MerTK was applied to VSMCs, all of the downstream signals of the TAM receptors including Akt/mTOR, ERK and FAK were partially suppressed. On the contrary, either ONO-7475, a dual AXL/MerTK inhibitor or combination treatment of bemcentinib (AXL inhibitor) and UNC2250 (MerTK inhibitor) almost completely blocked all of the downstream signals of the csEV-activated TAM receptors, and most potently suppressed VSMC proliferation and migration (Fig. 8). Furthermore, the sole treatment of bemcentinib or UNC2250 did not significantly inhibit the increase in AXL expression, whereas ONO-7475 treatment markedly suppressed AXL expression.

In summary, csEVs promote the proliferation and migration of VSMCs through AXL and MerTK. csEV-activated AXL and MerTK share the downstream signaling pathways of Akt, ERK and FAK that mediate the effects of csEVs. AXL expression is upregulated in the
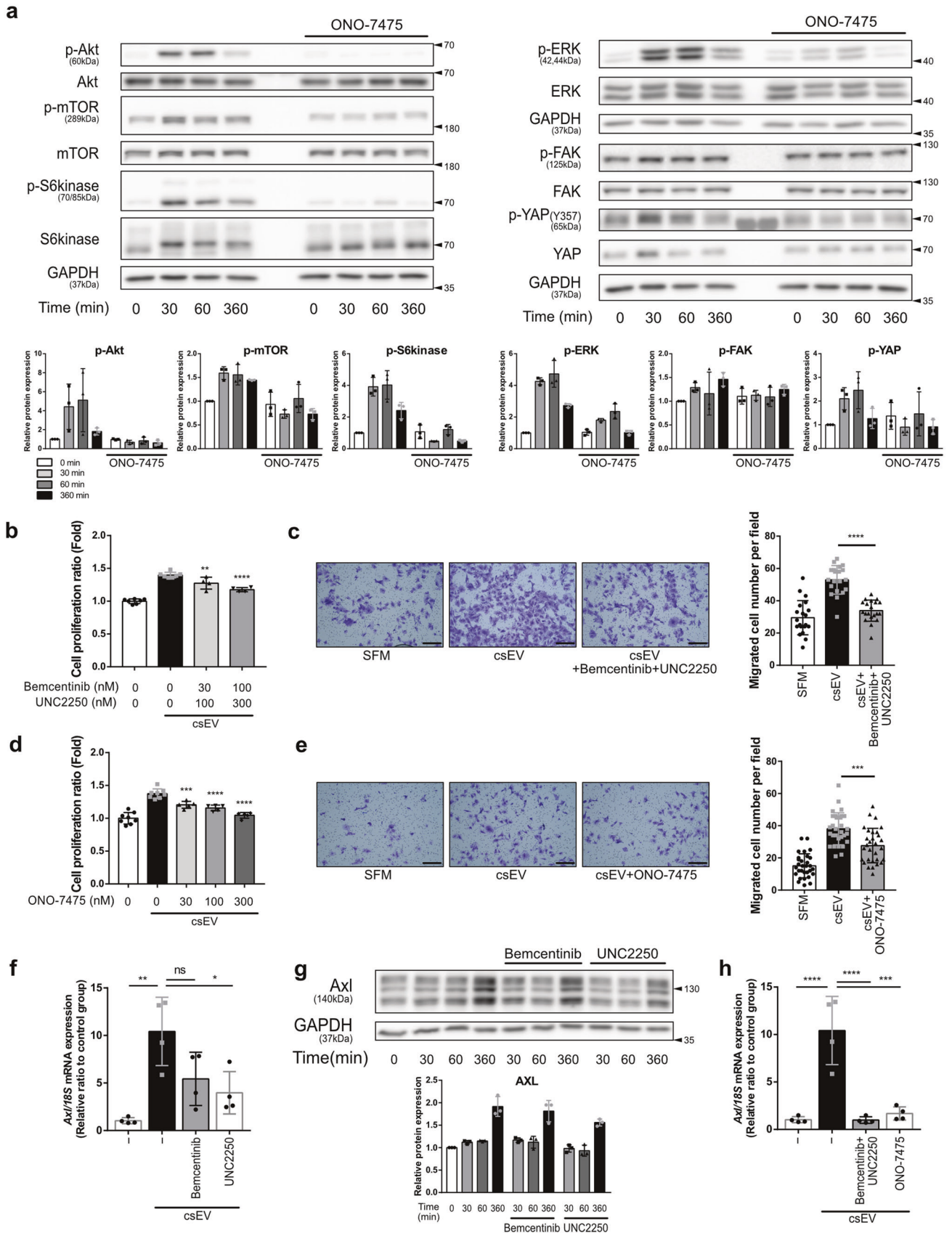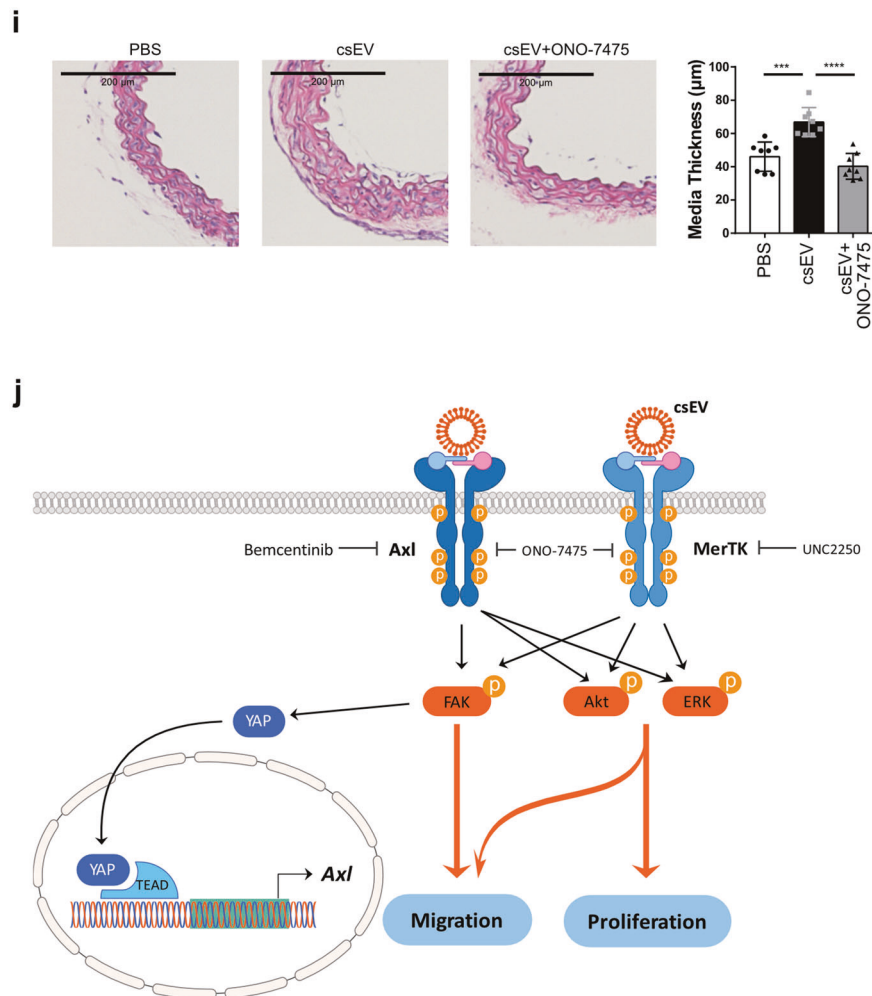
csEVs promote proliferation and migration of VSMCs
YJ Lee et al.

996

Fig. 8 (Continued).

csEVs promote proliferation and migration of VSMCs
YJ Lee et al.

997

Fig. 8 Dual inhibition of AXL and MerTK completely blocks csEV-induced proliferation and migration of VSMCs. a Effects of ONO-7475 (0.1 μM) on csEV-induced activation of Akt, ERK and FAK signaling pathways in VSMCs ($n = 3$). **b, c** VSMCs were treated with bemcentinib and UNC2250, or (**d, e**) ONO-7475 prior to incubation with csEV. **b, d** Relative proliferation rate was determined 48 h after exposure of VSMCs to csEV ($n = 4$–8), and (**c, e**) the number of migrated VSMCs was quantified in the Transwell assay 24 h after csEV exposure ($n = 20$–30; Scale bar, 200 μm). Effects of bemcentinib or UNC2250 on csEV-induced expression of (**f**) the mRNA level of *Axl* ($n = 4$) and (**g**) AXL protein expression in VSMCs ($n = 3$). **h** Effect of ONO-7475 on the csEV-induced *Axl* mRNA expression in VSMCs ($n = 4$). **i** H&E staining of mouse thoracic aortas 5 days after ex vivo vessel injury and treatment (Scale bar, 200 μm). The media thicknesses were calculated ($n = 8$). **j** Graphical illustration of csEV-stimulated proliferation and migration of VSMCs. Data represent means ± S.D. Statistical significance was determined using one-way ANOVA followed by Tukey-Kramer multiple-comparisons test. *$P < 0.05$; **$P < 0.01$; ***$P < 0.001$; ****$P < 0.0001$; ns, not significant, significant as compared to csEV-treated group or indicated group.

injured vascular wall. csEVs play a part in increasing the AXL level through FAK/YAP signaling, thereby possibly intensifying its own effects. These findings suggest dual AXL/MerTK inhibitors as potential therapeutic agents for inhibition of neointimal hyperplasia.

AUTHOR CONTRIBUTIONS
YJL: conceptualization, investigation, validation, writing - original draft. MP: writing - review and editing. HYK: writing - review and editing. JKK: resources. WKK: methodology. SCL: methodology. KWK: conceptualization, writing - review and editing, funding acquisition, supervision.

REFERENCES
1. Iqbal J, Gunn J, Serruys PW. Coronary stents: historical development, current status and future directions. Br Med Bull. 2013;106:193–211.
2. Ross R. The pathogenesis of atherosclerosis: a perspective for the 1990s. Nature. 1993;362:801–9.
3. Shi N, Chen SY. Smooth muscle cell differentiation: model systems, regulatory mechanisms, and vascular diseases. J Cell Physiol. 2016;231:777–87.
4. Rzucidlo EM, Martin KA, Powell RJ. Regulation of vascular smooth muscle cell differentiation. J Vasc Surg. 2007;45:A25–A32.

5. Bennett MR, Sinha S, Owens GK. Vascular smooth muscle cells in atherosclerosis. Circ Res. 2016;118:692–702.

6. Nishida-Aoki N, Tominaga N, Takeshita F, Sonoda H, Yoshioka Y, Ochiya T. Disruption of circulating extracellular vesicles as a novel therapeutic strategy against cancer metastasis. Mol Ther. 2017;25:181–91.

7. Jansen F, Nickenig G, Werner N. Extracellular vesicles in cardiovascular disease: potential applications in diagnosis, prognosis, and epidemiology. Circ Res. 2017;120:1649–57.

8. Raposo G, Stoorvogel W. Extracellular vesicles: exosomes, microvesicles, and friends. J Cell Biol. 2013;200:373–83.

9. Wang Z, Zhu H, Shi H, Zhao H, Gao R, Weng X, et al. Exosomes derived from M1 macrophages aggravate neointimal hyperplasia following carotid artery injuries in mice through miR-222/CDKN1B/CDKN1C pathway. Cell Death Dis. 2019;10:422.

10. Vajen T, Benedikter BJ, Heinzmann ACA, Vasina EM, Henskens Y, Parsons M, et al. Platelet extracellular vesicles induce a pro-inflammatory smooth muscle cell phenotype. J Extracell Vesicles. 2017;6:1322454.

11. Sorrentino TA, Duong P, Bouchareychas L, Chen M, Chung A, Schaller MS, et al. Circulating exosomes from patients with peripheral artery disease influence vascular cell migration and contain distinct microRNA cargo. JVS Vasc Sci. 2020;1:28–41.

12. Johnsen KB, Gudbergsson JM, Andresen TL, Simonsen JB. What is the blood concentration of extracellular vesicles? Implications for the use of extracellular vesicles as blood-borne biomarkers of cancer. Biochim Biophys Acta Rev Cancer. 2019;1871:109–16.

13. Wang Y, Xie Y, Zhang A, Wang M, Fang Z, Zhang J. Exosomes: an emerging factor in atherosclerosis. Biomed Pharmacother. 2019;115:108951.

14. Park M, Kim JW, Kim KM, Kang S, Kim W, Kim JK, et al. Circulating small extracellular vesicles activate TYRO3 to drive cancer metastasis and chemoresistance. Cancer Res. 2021;81:3539.

15. Linger RMA, Keating AK, Earp HS, Graham DK. TAM receptor tyrosine kinases: biologic functions, signaling, and potential therapeutic targeting in human cancer. Adv Cancer Res. 2008;100:35–83.

16. Melaragno MG, Fridell YWC, Berk BC. The Gas6/Axl system: a novel regulator of vascular cell function. Trends Cardiovasc Med. 1999;9:250–3.

17. Skotland T, Hessvik NP, Sandvig K, Llorente A. Exosomal lipid composition and the role of ether lipids and phosphoinositides in exosome biology. J Lipid Res. 2019;60:9–18.

18. Yan X, Doffek K, Yin C, Krein M, Phillips M, Sugg SL, et al. Annexin-V promotes anti-tumor immunity and inhibits neuroblastoma growth in vivo. Cancer Immunol Immunother. 2012;61:1917–27.

19. Krahling S, Callahan MK, Williamson P, Schlegel RA. Exposure of phosphatidylserine is a general feature in the phagocytosis of apoptotic lymphocytes by macrophages. Cell Death Differ. 1999;6:183–9.

20. Nakano T, Higashino K, Kikuchi N, Kishino J, Nomura K, Fujita H, et al. Vascular smooth muscle cell-derived, Gla-containing growth-potentiating factor for Ca^{2+}-mobilizing growth factors. J Biol Chem. 1995;270:5702–5.

21. Kasikara C, Kumar S, Kimani S, Tsou W-I, Geng K, Davra V, et al. Phosphatidylserine sensing by TAM receptors regulates AKT-dependent chemoresistance and PD-L1 expression. Mol Cancer Res. 2017;15:753.

22. Goruppi S, Ruaro E, Varnum B, Schneider C. Requirement of phosphatidylinositol 3-kinase-dependent pathway and Src for Gas6-Axl mitogenic and survival activities in NIH 3T3 fibroblasts. Mol Cell Biol. 1997;17:4442–53.

23. Hu Y-L, Lu S, Szeto KW, Sun J, Wang Y, Lasheras JC, et al. FAK and paxillin dynamics at focal adhesions in the protrusions of migrating cells. Sci Rep. 2014;4:6024.

24. Linger RM, Cohen RA, Cummings CT, Sather S, Migdall-Wilson J, Middleton DH, et al. Mer or Axl receptor tyrosine kinase inhibition promotes apoptosis, blocks growth and enhances chemosensitivity of human non-small cell lung cancer. Oncogene. 2013;32:3420–31.

25. Ghiso E, Migliore C, Ciciriello V, Morando E, Petrelli A, Corso S, et al. YAP-dependent AXL overexpression mediates resistance to EGFR inhibitors in NSCLC. Neoplasia. 2017;19:1012–21.

26. Mudduluru G, Leupold JH, Stroebel P, Allgayer H. PMA up-regulates the transcription of Axl by AP-1 transcription factor binding to TRE sequences via the MAPK cascade in leukaemia cells. Biol Cell. 2011;103:21–33.

27. Lachowski D, Cortes E, Robinson B, Rice A, Rombouts K, Del Rio Hernandez AE. FAK controls the mechanical activation of YAP, a transcriptional regulator required for durotaxis. FASEB J. 2018;32:1099–107.

28. Song X, Xu H, Wang P, Wang J, Affo S, Wang H, et al. Focal adhesion kinase (FAK) promotes cholangiocarcinoma development and progression via YAP activation. J Hepatol. 2021;75:888–99.

29. Lu Q, Lemke G. Homeostatic regulation of the immune system by receptor tyrosine kinases of the Tyro 3 family. Science. 2001;293:306–11.

30. Ye F, Li Q, Ke Y, Lu Q, Han L, Kaplan HJ, et al. TAM receptor knockout mice are susceptible to retinal autoimmune induction. Invest Ophthalmol Vis Sci. 2011;52:4239–46.

31. Togliatto G, Dentelli P, Rosso A, Lombardo G, Gili M, Gallo S, et al. PDGF-BB carried by endothelial cell–derived extracellular vesicles reduces vascular smooth muscle cell apoptosis in diabetes. Diabetes. 2018;67:704.

32. Otani K, Yokoya M, Fujioka Y, Okada M, Yamawaki H. Small extracellular vesicles from rat plasma promote migration and proliferation of vascular smooth muscle cells. J Vet Med Sci. 2020;82:299–306.

33. McShane L, Tabas I, Lemke G, Kurowska-Stolarska M, Maffia P. TAM receptors in cardiovascular disease. Cardiovasc Res. 2019;115:1286–95.

34. Jin CW, Wang H, Chen YQ, Tang MX, Fan GQ, Wang ZH, et al. Gas6 delays senescence in vascular smooth muscle cells through the PI3K/ Akt/FoxO signaling pathway. Cell Physiol Biochem. 2015;35:1151–66.

35. Korshunov Vyacheslav A. Axl-dependent signalling: a clinical update. Clin Sci. 2012;122:361.

36. Dagamajalu S, Rex DAB, Palollathil A, Shetty R, Bhat G, Cheung LWT, et al. A pathway map of AXL receptor-mediated signaling network. J Cell Commun Signal. 2021;15:143–8.

37. Cummings CT, DeRyckere D, Earp HS, Graham DK. Molecular pathways: MERTK signaling in cancer. Clin Cancer Res. 2013;19:5275.

38. Louis SF, Zahradka P. Vascular smooth muscle cell motility: from migration to invasion. Exp Clin Cardiol. 2010;15:e75–e85.

39. Jeong K, Kim J-H, Murphy JM, Park H, Kim S-J, Rodriguez YA, et al. Nuclear focal adhesion kinase controls vascular smooth muscle cell proliferation and neointimal hyperplasia through GATA4-mediated cyclin D1 transcription. Circ Res. 2019;125:152–66.

40. Melaragno MG, Wuthrich DA, Poppa V, Gill D, Lindner V, Berk BC, et al. Increased expression of Axl tyrosine kinase after vascular injury and regulation by G protein–coupled receptor agonists in rats. Circ Res. 1998;83:697–704.

41. Saab S, Chang OS, Nagaoka K, Hung MC, Yamaguchi H. The potential role of YAP in Axl-mediated resistance to EGFR tyrosine kinase inhibitors. Am J Cancer Res. 2019;9:2719–29.

42. Kimura TE, Duggirala A, Smith MC, White S, Sala-Newby GB, Newby AC, et al. The Hippo pathway mediates inhibition of vascular smooth muscle cell proliferation by cAMP. J Mol Cell Cardiol. 2016;90:1–10.